23. L. D. Ashwal, D. A. Morrison, W. C. Phinney, J. Wood, *Contrib. Mineral. Petrol.* **82**, 259 (1983).
24. R. L. Rudnick, *Geochim. Cosmochim. Acta* **56**, 963 (1992).
25. R. H. Hewins, *Proc. Lunar Planet. Sci. Conf. 15* [*J. Geophys. Res.* **89**, C289 (1984)].
26. M. B. Duke and L. T. Silver, *Geochim. Cosmochim. Acta* **31**, 1637 (1967).
27. B. N. Powell, *ibid.* **35**, 5 (1971).
28. F. Herbert, *Icarus* **78**, 402 (1989).
29. J. T. Wasson and A. E. Rubin, *Nature* **318**, 168 (1985).
30. F. Herbert, personal communication.
31. The REE data shown in Fig. 1 are from 35 literature sources too numerous to list here. A full listing of data sources is available from the senior author on request.
32. We thank J. Jones for reviewing an early version of the manuscript and F. Herbert for illuminating discussions on joule heating. This work was supported by the National Aeronautics and Space Administration through grants NAG 9-111 (A.M.D.), NAG 9-51 (R. N. Clayton), RTOP 152-13-40-21 (M. M. Lindstrom), and NAG 9-40 (J. T. Wasson).

2 April 1992; accepted 30 June 1992

Thermoelasticity of Silicate Perovskite and Magnesiowüstite and Stratification of the Earth's Mantle

Lars Stixrude,* R. J. Hemley, Y. Fei, H. K. Mao

Analyses of x-ray-diffraction measurements on (Mg,Fe)SiO_3 perovskite and (Mg,Fe)O magnesiowüstite at simultaneous high temperature and pressure are used to determine pressure-volume-temperature equations of state and thermoelastic properties of these lower mantle minerals. Detailed comparison with the seismically observed density and bulk sound velocity profiles of the lower mantle does not support models of this region that assume compositions identical to that of the upper mantle. The data are consistent with lower mantle compositions consisting of nearly pure perovskite (>85 percent), which would indicate that the Earth's mantle is compositionally, and by implication, dynamically stratified.

The lower mantle is the largest single region of the Earth's interior, accounting for 55% of its volume. In contrast to the case for the upper mantle, from which we have samples, we cannot determine the composition of the lower mantle by direct observation, yet its major element chemistry has important implications for the evolution of our planet and its current thermal and chemical state. The possibility of compositional stratification—distinct upper and lower mantle compositions—implies that the Earth's mantle convects in at least two layers and that the planet has evolved slowly and retained much of its primordial heat and large-scale geochemical heterogeneities. Despite its importance, the most direct approach to determining lower mantle composition, comparison of laboratory experiments with seismic observations, has been subject to substantial uncertainties, and the question of compositional stratification remains open. The greatest difficulty has been the acquisition of accurate measurements at the relevant conditions. Experiments have only recently achieved high temperatures at pressures greater than 1 bar and high pressures at temperatures greater than 300 K (*1*, *2*). In this report we present a thermodynamic analysis and the geophysical implications of these measurements.

Geophysical Laboratory and Center for High Pressure Research, Carnegie Institution of Washington, 5251 Broad Branch Road, N.W., Washington, DC 20015.

*Present address, School of Earth and Atmospheric Sciences, Georgia Institute of Technology, Atlanta, Georgia 30332.

Constraints on lower mantle composition can be obtained from accurate experimental measurements of thermoelastic properties of the constituent materials. This approach requires determination of the room temperature equation of state, the thermal expansivity, α, and the dimensionless Anderson-Grüneisen ratio

$$\delta_X = -\frac{K_X}{\alpha}\left(\frac{\partial \alpha}{\partial P}\right)_X = -\frac{1}{\alpha K_X}\left(\frac{\partial K_X}{\alpha T}\right)_P \quad (1)$$

where $X = T$ or S (temperature or entropy) P is pressure, and K_X is the isothermal or adiabatic bulk modulus. These quantities relate laboratory data to the density, ρ, and seismic parameter, $\Phi = K_S/\rho$, at pressure-temperature conditions of the lower mantle (*3*, *4*). For the purpose of illustration, we assume that δ_X is independent of P and T, yielding

$$\rho(P,T) = \rho(P,T_0)\exp[-\bar{\alpha}\Delta T] \quad (2)$$

$$\Phi(P,T) = \Phi(P,T_0)\exp[\bar{\alpha}(1 - \delta_S)\Delta T] \quad (3)$$

where $\Delta T = T - T_0$, and $\bar{\alpha} = \bar{\alpha}_0[\rho(0,T_0)/\rho(P,T_0)]^{\delta_T}$ is the mean value of $\alpha(P,T)$ from T_0 to T. There have been no earlier measurements of δ_T or δ_S of perovskite, and the pressure and temperature dependence of these quantities is not known. Several groups have measured the thermal expansivity of perovskite (*5*–*8*) but two of these studies disagree severely with each other (*5*, *8*). Workers analyzing lower mantle composition, relying on contradictory measurements or estimates of these crucial properties, have come to opposite conclusions. Some have argued for homogeneous mantle compositions (*8*–*10*) while others have proposed that the lower mantle is enriched in silica or iron, or both (*5*, *11*, *12*). Model calculations for a range of plausible values have indicated that values of $\bar{\alpha}_0$ greater than 2.5×10^{-5} to 4×10^{-5} K^{-1} and δ_T larger than 4 require that the lower mantle has a nearly pure perovskite composition (*9*, *13*).

Recently, the equations of state of $(Mg_{0.9},Fe_{0.1})SiO_3$ perovskite and $(Mg_{0.6},Fe_{0.4})O$ magnesiowüstite were measured at combined high pressures and temperatures (*1*, *2*) (Fig. 1). The measurements were performed in externally heated diamond cells with the use of synchrotron x-ray diffraction. These data place experimental constraints on the thermal expansivity of perovskite at high pressures; that is to within the stability field of the material (P > 23 GPa). Such data are particularly important for perovskite because of problems associated with its metastability at low pressure (*14*, *15*). The data show that thermal expansivity decreases strongly with pressure and increases strongly with temperature, so that $\bar{\alpha}_0$ (300 to 2000 K) is significantly larger than 4×10^{-5} K^{-1}. The value of δ_T ($\approx$7) was found to be substantially greater than earlier estimates (*1*), whereas the results for magnesiowüstite were consistent with earlier predictions (*2*, *16*). Detailed comparison with seismic determinations of ρ and Φ requires analysis of these quantities at lower mantle conditions.

We extract from the data the Debye temperature, θ_0, the Grüneisen parameter, γ_0, and q (*17*). These quantities are used to characterize the thermodynamic Helmholtz potential, $F(\rho,T)$, which yields complete thermodynamic information through its density and temperature derivatives (*18*). This approach allows us to calculate self-consistent equations of state and adiabatic temperature profiles, which are appropriate for a convecting system (Fig. 2). Possible systematic errors in the extrapolation of ρ and Φ to mantle conditions, due to the assumed form of $F(\rho,T)$, are expected to be small. Indeed, density and seismic parameter profiles determined from $F(\rho,T)$ with either Einstein or Debye models of the vibrational density of states are identical to Eqs. 2 and 3 with

constant δ_T and δ_S, within experimentally derived uncertainties (Fig. 1). As shown in Fig. 1, the pressure dependence of ρ and Φ for $(Mg,Fe)SiO_3$ perovskite at 2000 K calculated from the experimental data are close to the seismic observations. The data thus suggest that silicate perovskiteis predominant in the lower mantle relative to magnesiowüstite (and other phases).

To examine this hypothesis further, we compare seismic observations with a wide range of plausible compositions and mantle adiabats. The range of compositions is characterized by the bulk mole fractions of iron X_{Fe} = Fe/(Fe + Mg), and perovskite X_{Pv} = Pv/(Pv + Mw), and the geotherms are characterized by the temperature at the foot of the adiabat, T_0 (at 670 km depth or 24 GPa) (*19*). A pure perovskite composition (X_{Fe} = 0.12, X_{Pv} = 1, T_0 = 2000 K) best matches the observed density and seismic parameter profiles of the lower mantle (Fig. 3). This conclusion is also consistent with the measured values for $\bar{\alpha}_0$ and δ_T (Figs. 1 and 2).

The recent high pressure-temperature measurements place important constraints on the effects of temperature and composition on ρ and Φ profiles. These effects are illustrated by extreme cases that fall well outside calculated uncertainties, including iron-free perovskite, orthosilicate stoichiometry, and T_0 = 1000 K, which show that iron enrichment increases ρ and decreases Φ, silica enrichment increases both quantities, and increasing T_0 decreases both (Fig. 3). Variation of X_{Fe}, X_{Pv}, or T_0 separately is restricted to approximately 30%, but significant tradeoffs exist among the parameters (Fig. 3). Clearly, simultaneous enrichment in silica and iron and increases in temperature define a series of lower mantle assemblages with similar properties. These tradeoffs, however, are not unlimited. For example, increasing T_0 decreases densities much more at low pressures than at high pressures (Eq. 1), so that the range of density spanned by the calculated Φ-ρ curve over the same pressure interval increases. Enrichment in magnesiowüstite has a similar effect, because its density is less than that of perovskite at low pressure but greater at high pressure.

The full range of compositions that satisfy the seismic data is illustrated by the $\chi^2(X_{Fe},X_{Pv},T_0)$ surface (*20*). We show the section $\chi^2(X_{Fe},X_{Pv},T_0^*)$, where T_0^* yields the best fit for a given composition (Fig. 4). The form of the confidence regions reflects tradeoffs between composition and temperature. A composition of pure perovskite matches the data best, but perovskite fractions as low as 0.45 are permitted at the 68% (1σ) confidence level. Iron content is much more tightly constrained because it most strongly affects density, which has small calculated uncertainties. Typical upper mantle compositions (*21*)

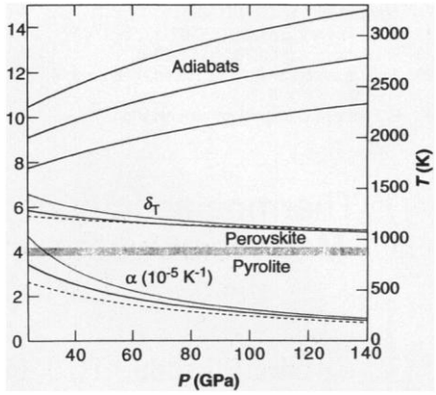

Fig. 2. Lower mantle adiabats (T_0 = 1700, 2000, 2300 K) for (X_{Pv} = 1, X_{Fe} = 0.12), and experimentally constrained values of δ_T and α along 1000 (dashed), 2000 (solid) and 3000 K (dotted) isotherms from $F(\rho,T)$. The uncertainty in δ_T is approximately 30%. The shaded horizontal bar separates values of δ_T consistent with a perovskite lower mantle composition from those consistent with upper mantle (pyrolite) compositions (*9*).

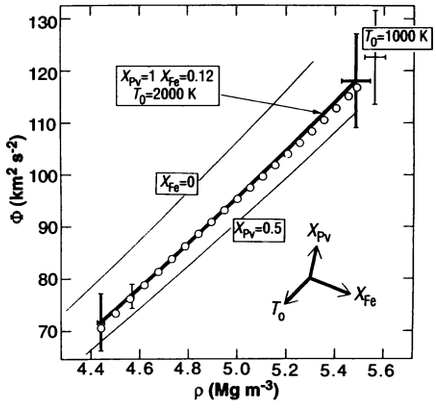

Fig. 3. Calculated values of density and seismic parameter over the pressure regime of the lower mantle (28.3 < P < 127.0 GPa) for the assemblage (X_{Fe} = 0.12, X_{Pv} = 1, T_0 = 2000 K) (bold line with error bars). Also shown are the assemblages (X_{Fe} = 0, X_{Pv} = 1, T_0 = 2000 K) and (X_{Fe} = 0.12, X_{Pv} = 0.5, T_0 = 2000 K), represented by the dashed lines, and (X_{Fe} = 0.12, X_{Pv} = 1, T_0 = 1000 K), represented by the light error bars at its end points. The symbols are the seismically observed values (*20*). The arrows show the direction that the calculated ρ-Φ curve shifts if the indicated parameter is increased. The zero pressure volume of perovskite is V_0 = 24.46 + 1.03 X_{Fe}. Magnesiowüstite parameters are V_0 = 11.25 ± 1.00 X_{Fe}, K_0 = 157 ± 2 GPa, K_0' = 4.0 ± 0.4, θ_0 = 500 ± 50 *K*, γ_0 = 1.50 ± 0.03, q = 1.1 ± 0.7 (*17*). The Fe-Mg partition coefficient between perovskite and magnesiowüstite, $K_{Pv\text{-}Mw}$ = 1/6 (*30*).

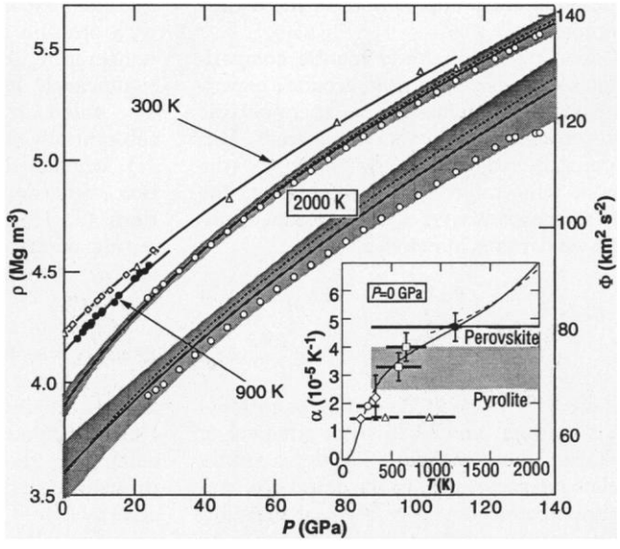

Fig. 1. Measured density of $(Mg_{0.9},Fe_{0.1})SiO_3$ perovskite versus pressure at room temperature [data marked ◇ is from (*1*) and △ is from (*28*)] and high temperature [● (*1*)]. High-temperature data are corrected to a common isotherm with $\bar{\alpha}_0 = 3.3 \times 10^{-5}$ K^{-1} and δ_T = 7. Lines are based on the Birch-Murnaghan equation of state with a zero pressure volume V_0 = 24.56 cm^3 mol^{-1}, isothermal bulk modulus K_0 = 263 ± 7 GPa, and its pressure derivative K_0' = 3.9 ± 0.4 (*17*). Solid lines are from $F(\rho,T)$ with θ_0 = 1017 ± 7 K, γ_0 = 1.96 ± 0.10, q = 2.5 ± 1.7 (*15*). Dashed lines are from Eqs. 2 and 3 with $\bar{\alpha}_0 = 4.7 \times 10^{-5}$ K^{-1}, δ_T = 7 and δ_S = 3. δ_T and δ_S are closely related: assuming that αK_T is independent of T, a good approximation for T above the Debye temperature, $\delta_S = \delta_T - \gamma\,[1 + \alpha(q + \delta_T)T]/(1 + \alpha\gamma T)$. The data are compared with the density and seismic parameter of the lower mantle (○) (20). The inset compares $\alpha(T)$ and $\bar{\alpha}_0$ determined from the data [● (*1*)] with previously reported values [data marked □ is from (*5, 29*), ◇ is from (*6*), ○ is from (*7*), and △ is from (*8*)]. Vertical bars are uncertainties as quoted by the authors, horizontal bars show the range over which α was averaged. The shading separates values of $\bar{\alpha}_0$ which are consistent with a perovskite lower mantle composition from those consistent with upper mantle (pyrolite) compositions (*9, 13*). Thermal expansivity, $\alpha(T)$ is calculated from $F(\rho,T)$ (solid line) and $\alpha = (B/K_0)[\rho(0,T_0/\rho(0,T)]^{\delta_T}$ (dashed line), where $B = \alpha K_T$ [10.2 MPa K^{-1} (*1*)] is assumed to be independent of temperature above the Debye temperature.

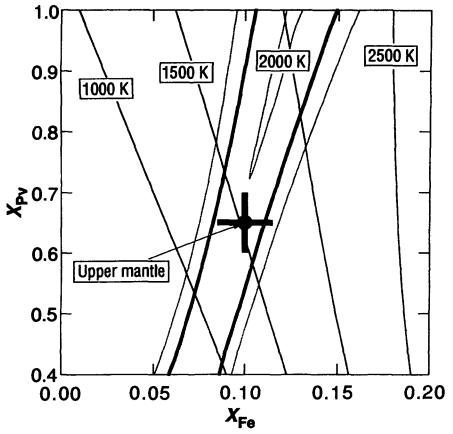

Fig. 4. Combined misfit to seismically observed ρ and Φ profiles as represented by the $\chi^2(X_{Fe}, X_{Pv}, T_0^*)$ surface showing 1σ (bold line) 2σ and σ/75 (dashed lines) confidence regions. The light solid lines are contours of T_0^*. The uncertainty in T_0^* is 100 K (1σ). The range of upper mantle compositions is indicated (*21*).

provide acceptable fits to the seismic data but only along adiabats which are unreasonably cold ($T_0 \approx 1500$ K) (*22*). Only compositions enriched in silica and iron match the seismic data along plausible mantle adiabats: $T_0 = 1700$ to 2100 K in the case of whole mantle convection or 2200 to 2600 K for two-layer convection (*22*, *23*). The thermal boundary layer implied by a different lower mantle composition and two-layer convection requires a nearly pure perovskite composition (>85%).

The extent to which this conclusion is affected by the presence of minor elements, including Ca and Al, possible phase transitions in perovskite and magnesiowüstite, and variation in δ_T at still higher pressure-temperature conditions will require additional experimental investigation (*24*). The change in chemical composition between upper and lower mantle implied by the results may not coincide with the 670-km discontinuity, which is caused by a change in phase. Although the 670-km discontinuity is thermodynamically controlled—its small lateral variations in depth (*25*) (<30 km) are determined by the Clapeyron slope of perovskite forming reactions (*26*)—the compositional boundary is dynamically controlled and is expected to be deflected by 100 to 300 km in subduction zones (*4*). The velocity contrast across a purely compositional change is expected to be small (*27*). Unless it is diffuse, reflections from a compositional boundary may be observable as companions to the much stronger 670 km signal in subduction zones. Seismic detection of such a boundary would provide significant additional constraints on mantle stratification.

REFERENCES AND NOTES

1. H. K. Mao *et al.*, *J. Geophys. Res.* **96**, 8069 (1991).
2. Y. Fei, H. K. Mao, J. Shu, J. Hu, *Phys. Chem. Minerals* **18**, 416 (1992).
3. Inversion of a large body of data, including body wave travel times and free oscillation frequencies, yields spherically averaged (one-dimensional) profiles of the density and seismic parameter of the lower mantle that are known to within 0.5% [see (*4*)] and 1% [R. C. Lee and L. R. Johnson, *Geophys. J. R. Astron. Soc.* **77**, 667 (1984)], respectively, based on formal resolution analyses.
4. P. G. Silver, R. W. Carlson, P. Olson, *Annu. Rev. Earth Planet. Sci.* **16**, 477 (1988), and references therein.
5. E. Knittle, R. Jeanloz, G. L. Smith, *Nature* **319**, 214 (1986).
6. N. L. Ross and R. M. Hazen, *Phys. Chem. Minerals* **16**, 415 (1989).
7. J. B. Parise, Y. Wang, A. Yeganeh-Haeri, D. E. Cox, Y. Fei, *Geophys. Res. Lett.* **17** (1990).
8. Y. Wang *et al.*, *Science* **251**, 410 (1991).
9. M. S. T. Bukowinski and G. H. Wolf, *J. Geophys. Res.* **95**, 12583 (1990).
10. E. Ito, E. Takahashi, Y. Matsui, *Earth Planet. Sci. Lett.* **67**, 238 (1984); A. Chopelas and R. Boehler, *Geophys. Res. Lett.* **16**, 1347 (1989).
11. R. Jeanloz and E. Knittle, *Philos. Trans. R. Soc. London Ser. A* **238**, 377 (1989).
12. D. L. Anderson and J. D. Bass, *Nature* **320**, 321 (1986); R. Jeanloz and E. Knittle, *Adv. Phys. Geochem.* **6**, 275 (1986); C. R. Bina and P. G. Silver, *Geophys. Res. Lett.* **17**, 1153 (1990).
13. I. Jackson, *Earth Planet. Sci. Lett.* **62**, 91 (1983); R. Jeanloz and A. B. Thompson, *Rev. Geophys. Space Phys.* **21**, 51 (1983).
14. R. J. Hemley and R. E. Cohen, *Annu. Rev. Earth Planet. Sci.* **20**, 553 (1992).
15. The measurements of (*8*), which yield a significantly lower thermal expansivity, may be associated with degradation of the sample at the highest temperatures due to metastability (P = 7.3 GPa); see discussion in (*14*). A metastable phase transition was also reported (*8*) at 600 K at this pressure (that is, well below the stability field of perovskite). Mao *et al.* (*1*) found no evidence of a phase transition over the pressure-temperature range of that study (298 to 900 K and 0 to 30 GPa). Subsequent high-temperature diamond-cell studies below 10 GPa have also failed to reveal a transition [Y. Fei, in preparation]. The change may be an artifact associated with texturing (*14*). Phase transitions to tetragonal and cubic perovskite structures at higher temperatures and pressures (T > 900 K and P > 20 GPa) are possible [Y. Wang, F. Guyot, A. Yeganeh-Haeri, R. C. Liebermann, *Science* **248**, 468 (1990)]; these are expected to increase $\bar{\alpha}_0$ because of the larger volume of the high-symmetry phases (*14*), and hence increase the amount of silica and iron enrichment, with respect to upper mantle compositions, necessary to match the properties of the lower mantle.
16. See D. G. Isaak, O. L. Anderson, T. Goto, *Phys. Chem. Minerals* **16**, 704 (1989).
17. Thermodynamic parameters of magnesiowüstite are from (*2*); those of perovskite are from R. J. Hemley, L. Stixrude, Y. Fei, and H. K. Mao [in *High Pressure Research in Mineral Physics: Applications to Earth and Planetary Science*, Y. Syono and M. H. Manghnani, Eds. (Terrapub, Tokyo, in press)], which also describes how uncertainties in the parameters for both minerals were determined. γ and $-q$ are the first and second logarithmic density derivatives of θ.
18. L. Stixrude and M. S. T. Bukowinski, *J. Geophys. Res.* **95**, 19311 (1990).
19. The elastic properties of composites are inherently uncertain, but must lie between Voight and Reuss approximations [J. P. Watt, G. F. Davies, R. J. O'Connell, *Rev. Geophys.* **14**, 541 (1976)]. We estimated the seismic parameter of perovskite magnesiowüstite composites by the usual Hill average of these bounds. For X_{Pv} = 0.5, the bounds differ from the mean by an average of 0.3%.
20. $\chi^2(X_{Fe}, X_{Pv}, T_0)$
$$= \sum_{i=1}^{21} (\rho_i - \rho(P_i, T_i))^2/\sigma_\rho^2 + (\Phi_i - \Phi(P_i, T_i))^2/\sigma_\Phi^2$$
where ρ_i and Φ_i are the observed properties, ρ and Φ are calculated at the corresponding pressure and adiabatic temperature. The variances σ_ρ^2 and σ_Φ^2 are the sum of the variance in the observed seismic properties (*3*) and the variance in the calculated properties, including that due to (i) propagation of experimental errors (see Fig. 1), (ii) possible systematic errors in the thermodynamic model, which we estimate from the maximum difference between results based on $F(\rho, T)$ and Eqs. 2 and 3 (see Fig. 1), and (iii) composite-mixing effects (*19*). The sum, over the points in the PREM model of A. M. Dziewonski and D. L. Anderson [*Phys. Earth Planet. Int.* **25**, 297 (1981)], excludes the anomalous upper and lower few hundred kilometers of the lower mantle.
21. The range X_{Pv} = 0.65 ± 0.06, X_{Fe} = 0.1 ± 0.02, encompasses compositions that have been proposed for the upper mantle including pyrolite, piclogite, peridotite, and lherzolite [see, for example, A. E. Ringwood, *Composition and Petrology of the Earth's Mantle* (McGraw-Hill, New York, 1975); D. L. Anderson, *Theory of the Earth* (Blackwell, Boston, 1989)].
22. The temperature at a depth of 400 km (1700 ± 100 K) is determined by experimental observations of the transition of $(Mg,Fe)_2SiO_4$ olivine to wadsleyite; this transition is expected to cause the seismic discontinuity at this depth. Geothermometry and geobarometry of mantle-derived xenoliths, which indicate that the temperature at 200 km depth is 1600 ± 200 K, are consistent with this estimate. The temperature at the top of the lower mantle is estimated from the adiabatic gradient in the transition zone (depths of 400 to 670 km depth); inclusion of the effects of endothermic and exothermic phase changes yields 1700 to 2100 K for whole mantle convection or 2200 to 2600 K if the upper and lower mantles convect separately. See (*11*) and R. Jeanloz and S. Morris [*Annu. Rev. Earth Planet. Sci.* **14**, 377 (1986)].
23. C. R. Bina and R. J. Hemley, in preparation.
24. The presence of hitherto undiscovered high-pressure phases, associated with a lower mantle composition markedly different from that of the upper mantle, remains a perennial question and cannot be ruled out (*23*). However, experiments carried out to date indicate that the effect of minor elements on the bulk density is small at lower mantle pressures [for example, on a natural peridotite, B. O'Neill and R. Jeanloz, *Geophys. Res. Lett.* **17**, 1477 (1990)].
25. M. A. Richards and C. W. Wicks, *Geophys. J. Int.* **101**, 1 (1990); J. Revenaugh and T. H. Jordan, *J. Geophys. Res.* **96**, 19763 (1991); P. M. Shearer and T. G. Masters, *Nature* **355**, 791 (1992).
26. E. Ito and E. Takahashi, *J. Geophys. Res.* **94**, 10637 (1989).
27. R. Jeanloz, *Geophys. Res. Lett.* **18**, 1743 (1991).
28. E. Knittle and R. Jeanloz, *Science* **235**, 668 (1987).
29. Q. Williams, E. Knittle, R. Jeanloz, in *Perovskite: A Structure of Great Interest to Geophysics and Materials Science*, A. Navrotsky and D. J. Weidner Eds. (American Geophysical Union, Washington, DC, 1989), p. 1.
30. Y. Fei, H. K. Mao, B. O. Mysen, *J. Geophys. Res.* **96**, 2157 (1991).

31. We thank R. Jeanloz, R. E. Cohen, C. Lithgow-Bertelloni and an anonymous reviewer for helpful comments on the manuscript. This work is supported by National Science Foundation grants EAR-8916754 and EAR-9117858.

28 April 1992; accepted 15 July 1992